

Influence of Fluorosubstitution on the Structure of Zinc Phthalocyanine Thin Films

Darya D. Klyamer,^{a,b} Aleksandr S. Sukhikh,^{a,b} Sergey A. Gromilov,^{a,b} Vladimir N. Kruchinin,^c Evgeniy V. Spesivtsev,^c Aseel K. Hassan,^d and Tamara V. Basova^{a,b@}

^aNikolaev Institute of Inorganic Chemistry SB RAS, 630090 Novosibirsk, Russia

^bNovosibirsk State University, 630090 Novosibirsk, Russia

^cRzhanov Institute of Semiconductor Physics SB RAS, 630090 Novosibirsk, Russia

^dMaterials and Engineering Research Institute, Sheffield Hallam University, Sheffield, UK

@Corresponding author E-mail: basova@niic.nsc.ru

In this work, thin films of tetrafluorosubstituted zinc phthalocyanine (ZnPcF₄) were deposited by organic molecular beam deposition and studied to reveal the effects of F-substituents on the ZnPcF₄ single crystals and thin films structure. A combination of spectral ellipsometry, atomic force microscopy and diffraction techniques has been used to elucidate the structural features and molecular orientation of thin films of ZnPcF₄. Structural features of the films grown by co-evaporation of ZnPc and ZnPcF₄ (1:1) were also considered. Both ZnPcF₄ and ZnPc/ZnPcF₄ films have a preferred orientation along (001) plane with inclination angle of molecules relative to the substrate surface equal to 80° and the lower degree of crystallinity compared to the ZnPc film.

Keywords: Zinc phthalocyanines, thin films, orientation, crystal structure.

Влияние фторзамещения на структуру тонких пленок фталоцианината цинка

Д. Клямер,^{a,b} А. Сухих,^{a,b} С. Громилов,^{a,b} В. Кручинин,^c Е. Спесивцев,^c А. Хассан,^d Т. Басова^{a,b@}

^aИнститут неорганической химии им. А.В. Николаева СО РАН, 630090 Новосибирск, Россия

^bНовосибирский национальный исследовательский государственный университет, 630090 Новосибирск, Россия

^cИнститут физики полупроводников им. А.В. Ржанова СО РАН, 630090 Новосибирск, Россия

^dИнститут материалов и машиностроения, Шеффилд Халлам Университет, Шеффилд, Великобритания

@E-mail: basova@niic.nsc.ru

В настоящей работе проводится исследование тонких пленок тетрафторзамещенного фталоцианината цинка (ZnPcF₄), полученных методом осаждения из молекулярного пучка в вакууме. Для выявления влияния F-заместителей во фталоцианиновом кольце на структуру монокристалла и тонких пленок ZnPcF₄ проведено их сравнительное исследование с незамещенным аналогом ZnPc. Для исследования структурных особенностей и ориентации пленок использовалась комбинация методов спектральной эллипсометрии, атомной силовой микроскопии и рентгеновской дифракции. Кроме того, было проведено исследование пленок, полученных совместным испарением ZnPc и ZnPcF₄ (1:1). Пленки ZnPcF₄ и ZnPc/ZnPcF₄ характеризовались преимущественной ориентацией кристаллитов вдоль направления (001) и углом наклона молекул относительно поверхности подложки 80° и имели более низкую степень кристалличности по сравнению с пленками ZnPc.

Ключевые слова: Фталоцианинаты цинка, тонкие пленки, ориентация, кристаллическая структура.

Introduction

Thin films of both unsubstituted and substituted metal phthalocyanine (MPc) derivatives are of considerable interest as active layers of chemical sensors^[1,2] and field effect transistors.^[3–5]

Introduction of various substituents into the phthalocyanine macrocycle can significantly alter thin films structure and morphology and in its turn leads to the change of their electrical and sensing properties.^[6–11] Introduction of electron withdrawing fluorine substituents has been shown to change the molecular packing both in single crystals^[12–14] and in thin films^[15] compared to unsubstituted phthalocyanines. The structure of MPcF₁₆ (M=Cu, Co, Zn) single crystals grown by vacuum evaporation was found to be triclinic, with two molecules per unit cell and herringbone stacking.^[13–14] Single crystals of unsubstituted MPcs grown at the same experimental conditions are monoclinic with herringbone arrangement of phthalocyanine macrocycles.^[16]

It is well known that in the case of unsubstituted M(II) Pcs, the substrate temperature during deposition affects the morphology, phase composition and ordering of thin films. In the case of MPcF₁₆ (M=Co, Cu) films, it was shown that the substrate temperature and post-deposition annealing also cause the change of films morphology,^[3,17] however CuPcF₁₆ films exhibit the same phase composition independently of the deposition temperature.^[15] Morphology and structure of MPcF₁₆ films are dependent on their thickness.^[18] Yang *et al.* have shown that caterpillar-like crystal structure changes to nanobelt structure when thickness of the films becomes more than 30 nm.

F-substituents decrease the electron density of the aromatic ring and increase the oxidation potential of the MPc molecule.^[19] As a result, fluorosubstituted phthalocyanines exhibit the higher sensor response to such reducing gases as ammonia and hydrogen.^[16] The better sensor response of ZnPcF₁₆ and PdPcF₁₆ films towards gaseous ammonia compared to their unsubstituted analogues was shown by Schollhorn *et al.*^[20–21] and Klyamer *et al.*,^[6] respectively. It is well known that optical, electrical and sensing properties the phthalocyanine films might differ significantly in dependence on their structure and ordering.^[6,8] Moreover, fluorosubstituted metal phthalocyanines are used as *n*-type semiconductors for the preparation of ambipolar devices, *e.g.* organic field effect transistors, in combination with unsubstituted metal phthalocyanines or other organic molecules in bilayer architectures or as blends.^[4,9,10] For this reason the detailed study of structural features of fluorinated phthalocyanine films grown under different experimental conditions is an important task of materials chemistry.

To the best of our knowledge, only sporadic data on structure and properties of tetrafluorosubstituted metal phthalocyanine (MPcF₄) films are available in the literature.^[6–7,22] Schlettwein *et al.*^[22] analyzed the influence of fluorination degree in ZnPcF_x (x=0, 4, 8, 16) films on their optical and electrical properties. Schwarze *et al.*^[23] studied thin films of ZnPcF_x (x=4, 8, 16) co-evaporated with ZnPc onto glass substrates in various mixing ratios. Ultra thin films of CuPcF₄ on gold and ITO surfaces were studied by photoemission spectroscopy.^[24–25] Structural features and sensor

response of CoPcF₄ films toward ammonia were studied by Klyamer *et al.*^[6] Structure of single crystals of PdPcF₄ has been published in our recent work.^[7] The parameters of crystal cell of MPcF₄ (M=Cu, Zn) were reported by Jiang *et al.*,^[11] however the authors did not give the full data of single crystal structures and did not deposit the crystallographic data in the Cambridge Crystallographic Data Centre (CCDC). The detailed investigation of the structure and ordering of MPcF₄ films has also not yet been described in the literature.

In this work, thin films of tetrafluorosubstituted zinc phthalocyanine (ZnPcF₄) were deposited by organic molecular beam deposition (OMBD) and studied to reveal the effects of F-substituents on the ZnPcF₄ thin films structure. The crystalline structure of ZnPcF₄ single crystals has been refined using X-ray diffraction (XRD) measurements and their crystallographic data have been deposited in the Cambridge Crystallographic Data Centre with the reference number 1818040. A combination of spectral ellipsometry, atomic force microscopy (AFM) and XRD techniques have been used to elucidate the structural features and molecular orientation of thin films of ZnPcF₄. Structural features of the films grown by co-evaporation of ZnPc and ZnPcF₄ (1:1) are also considered.

Experimental

ZnPcF₄ was synthesized by heating a 4:1 mixture of 4-fluorophthalonitrile (Aldrich) and anhydrous zinc(II) chloride in a glass tube at 220 °C during 6 hours. The resulted product was purified by gradient sublimation in vacuum (10⁻⁵ Torr) at 450 °C. ZnPcF₄ was prepared as a statistical mixture of four regioisomers due to the various possible positions of fluorine substituents. No attempt was made to separate the ZnPcF₄ isomers. ZnPc (Aldrich) was also purified by gradient sublimation in vacuum (10⁻⁵ Torr) at 450 °C.

The ZnPc and ZnPcF₄ thin films were prepared by an OMBD technique at the substrate temperature of 60 °C. The evaporation was performed at a residual pressure of 10⁻⁵ Torr. The deposition rate was 0.6 nm·s⁻¹. The mixed films (further referred to as ZnPc/ZnPcF₄ film) were obtained by co-evaporation of ZnPc and ZnPcF₄ (1:1) at the same conditions. The chemical composition of the mixed films was determined by X-ray photoelectron spectroscopy (XPS) using a Phoibos-150 SPECS spectrometer (monochromatic AlK α -radiation, beam diameter *ca.* 1 mm).

The dispersive refractive indexes $N(\lambda)=n(\lambda)-k(\lambda)i$ and thicknesses for ZnPc and ZnPcF₄ films were obtained as a function of wavelength λ by means of spectroscopic ellipsometry. The spectral dependences of ellipsometric parameters Ψ and Δ were carried out using spectroscopic ellipsometer ELLIPS 1771 SA (ISP, Novosibirsk, Russia) over the range of $\lambda=250-1100$ nm.^[26] The spectral resolution of the instrument was 2 nm; the light beam angle of incidence was 70°. The solution of the inverse problem of ellipsometry and fitting of the spectral dependences of ellipsometric angles $\Psi(\lambda)$ and $\Delta(\lambda)$ were performed in accordance with the basic equation of ellipsometry:

$$\operatorname{tg}\Psi \cdot e^{-i\Delta} = R_p / R_s, \quad (1)$$

where R_p and R_s are the p- and s-components of the complex Fresnel reflection coefficients, respectively.^[27] In the calculations, the model of reflecting system “substrate – uniform film – air” was employed. Thus, in the whole spectral range, the spectral dependences of polarization angles were fitted for

each point of the spectrum independently by the error function minimization:

$$\sigma^2 = \left(\frac{\Delta_{exp.} - \Delta_{calc.}}{\delta\Delta_{err.}} \right)^2 + \left(\frac{\Psi_{exp.} - \Psi_{calc.}}{\delta\Psi_{err.}} \right)^2 \quad (2)$$

where $\Psi_{exp.}$, $\Delta_{exp.}$ and $\Psi_{calc.}$, $\Delta_{calc.}$ are experimental and calculated values of the ellipsometric parameters, while $\delta\Psi_{err.}$, $\delta\Delta_{err.}$ are experimental error values. Previously the film thickness was obtained at wavelength $\lambda=500$ nm ($k=0$). Solution of the multiangle ellipsometric (MAE) inverse problem was carried out in the framework of the model "Si substrate – uniform film – air". Then the thickness values were used in the dispersive optical parameter calculations.

AFM in tapping mode with a Nanoscope IIIa (Veeco Instruments, Plainview, U.S.A.) scanning probe microscope was used for films morphology characterization. UV-Vis spectra of ZnPc and ZnPcF₄ solutions and films on quartz substrates were recorded using a UV-Vis-NIR scanning spectrophotometer (UV-Vis-3101PC "Shimadzu"). Raman spectra were collected using a LabRAM HR Evolution (Horiba) spectrometer with the excitation by the 488 nm line of the Ar laser. IR spectra were recorded using a Vertex 80 FTIR spectrometer.

X-ray structure determination of ZnPcF₄ was carried out using a Bruker DUO single crystal diffractometer (4-circle kappa-goniometer, Mo-anode sealed tube, graphite monochromator, Apex II CCD area-detector, 1024×1024 pixels with 60 μm pixel size) using conventional phi- and omega-scans (0.5° wide). Sample temperature was kept at 160K by Oxford Cryosystems Cobra nitrogen open-flow cooler. X-ray diffraction patterns for polycrystalline powders were obtained at room temperature using Shimadzu XRD-7000 powder diffractometer (Cu-anode sealed tube, Ni-filter, Bragg-Brentano geometry, θ - θ goniometer, scintillation counter). Thin films samples were studied using combination of a XRD-7000 diffractometer for standard powder patterns and Bruker DUO diffractometer (Incoatec I μ Cu micro-focus source, 0.6 mm monocapillary focusing collimator) for 2D GIXD (2D Grazing incidence X-ray diffraction) patterns using a special sample adaptor. The primary beam angle of incidence was in the range from 0.3 to 0.5°. The distance from the sample to the CCD detector was 80 mm. This method has already been described^[28–29] in more details.

Results and Discussion

Structure of ZnPcF₄ Single Crystals

Single crystals of ZnPcF₄ were obtained by sublimation of the respective polycrystalline powder in a gradient furnace at 450 °C for 2 hours under vacuum (residual pressure $\sim 2 \cdot 10^{-5}$ Torr). An optical image of the obtained crystals is shown in Figure 1. Crystallographic data for ZnPcF₄ have been deposited in the Cambridge Crystallographic Data Centre (CCDC) with the reference number 1818040. ZnPcF₄ formed dense clusters of needle-shaped crystals with dark violet color and metallic shine, which is typical for unsubstituted and fluorinated phthalocyanines.^[14]

X-ray diffraction patterns for ZnPc and ZnPcF₄ polycrystalline powders obtained in the range from 2.5 to 40° 2 θ are shown in Figure 2. The ZnPc powder pattern fully coincides with the calculated one on the basis of the known β -ZnPc structural data^[30] (monoclinic $P2_1/a$, $a=19.274(5)$, $b=4.8538(15)$, $c=14.553(4)$ Å, $\beta=120.48(2)^\circ$). The ZnPcF₄ powder pattern is similar to that of CoPcF₄ and PdPcF₄^[6,7] and has single phase composition. Crystal structure

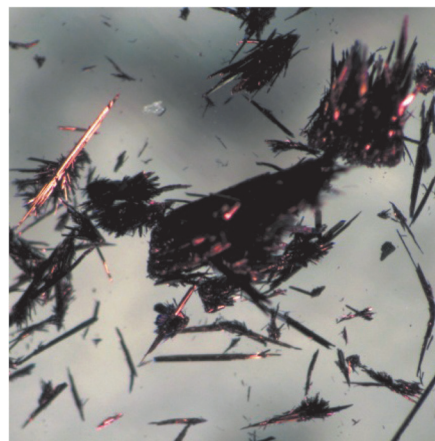


Figure 1. Microscopic image of ZnPcF₄ crystals.

of ZnPcF₄ was determined by the means of single crystal X-ray diffraction. A small (250×20×15 μm) needle-shaped crystal was mounted on a nylon loop with liquid epoxy. The Bruker APEX II software package (SAINT, SADABS)^[31] was used for indexing, collecting raw data, integration of diffraction reflections, global unit cell refinement and absorption correction. The resulting dataset was processed in Olex2 v1.2.9,^[32] with SHELXT-2014/5^[33] and SHELXL-2017/1^[34] used for structure determination and subsequent refinement. All non-hydrogen atom positions were refined anisotropically, without additional restraints. Fluorine atoms occupancy was refined as a free variable, based on the assumption that the total occupancy for two neighbouring positions should be equal to 1. The resulting occupancy values are 0.478/0.522 for F1 and F2 and 0.438/0.562 for F3 and F4, respectively (see Figure 3a).

The noticeable deviation from 0.5 is apparently caused by uneven proportions of ZnPcF₄ isomers. Hydrogen atoms were refined using the aromatic/amide riding coordinates. Since fluorine atoms occupy 8 peripheral positions only partially, hydrogen atoms with the complementary occupancy were added to the structure, therefore the total occupancy of each peripheral position is equal to one. Unit cell parameters and details of the structure refinement are given in Table 1.

Packaging diagrams for ZnPcF₄ are shown in Figure 3b. ZnPcF₄ molecule retains relatively flat conformation with all carbon, nitrogen and fluorine atoms deviating out of mean squared plane no more than 0.15 Å. The angles between peripheral benzene rings and the central macrocycle are 1.6° and 6.2°. ZnPcF₄ molecules are packed similarly to low-temperature metastable α -phases of unsubstituted M(II)Pcs (M=Co, Cu),^[35] PdPcF₄^[7] and CuPcF₄^[11] with $Z=1$, triclinic system and $P-1$ space group, however the space group and its unit cell parameters differ from those determined for ZnPcF₄ by Jiang *et al.*^[11] The distance between individual ZnPcF₄ molecules within a stack is 3.33 Å (3.41 Å for α -CoPc, 3.44 Å for α -CuPc and 3.37 Å for PdPcF₄), with 3.68 Å between the neighbouring Zn atoms and with the stacking angle (the angle between the least squares plane of the molecule and the line going through Zn atoms within a stack) $\theta=25.31^\circ$ (24.58° for α -CoPc, 25.21° for α -CuPc and 23.44° for PdPcF₄).

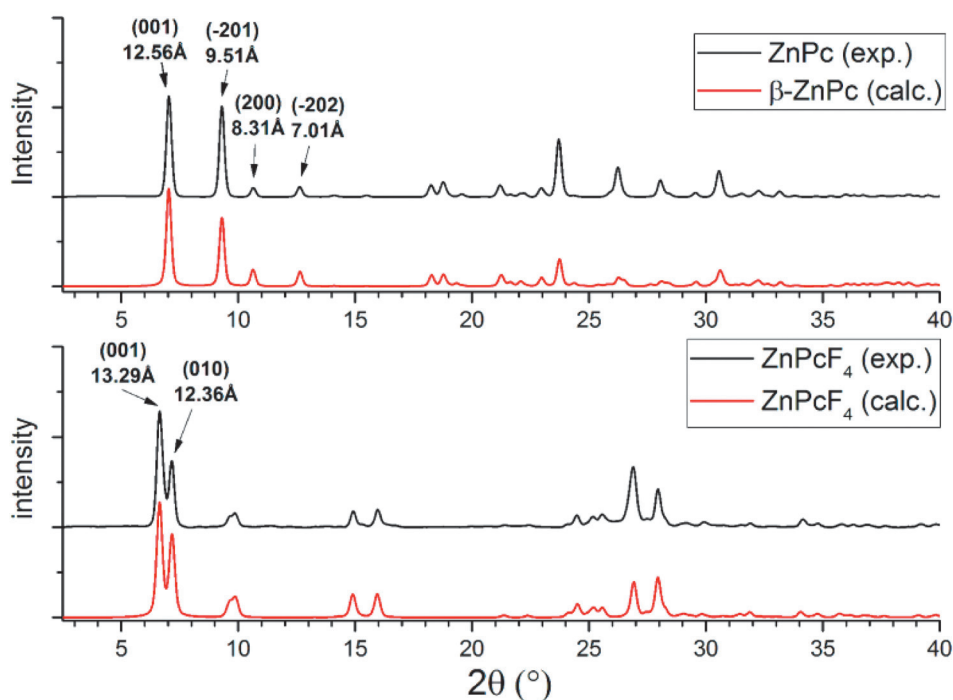


Figure 2. Diffraction patterns for ZnPc and ZnPcF₄ polycrystalline powders (Shimadzu XRD-7000, CuK_α-radiation, Bragg-Brentano geometry).

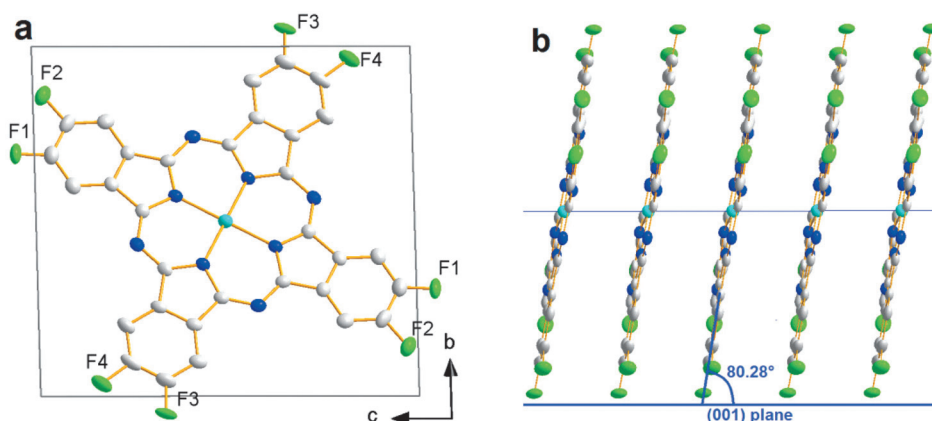


Figure 3. Packaging diagrams for ZnPcF₄: as viewed along axis (a) and along (001) lattice plane (b). Occupancy values are 0.478/0.522 for F1 and F2 and 0.438/0.562 for F3 and F4, respectively.

Study of ZnPc and ZnPcF₄ Thin Films

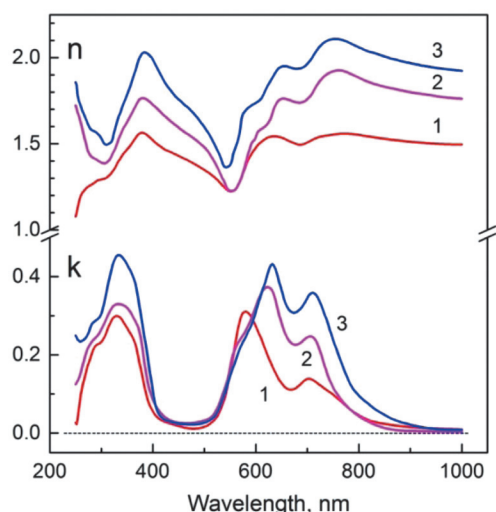
Dispersion dependences of the refractive index $n(\lambda)$ and the extinction coefficient $k(\lambda)$ calculated from the $\Psi(\lambda)$, $\Delta(\lambda)$ ellipsometric angle dependences for ZnPc, ZnPcF₄ and mixed ZnPc/ZnPcF₄ films are shown in Figure 4. There are two groups of the absorbance maxima in the spectra of the films which are typical for the most metal phthalocyanines:^[36–37] the broad *B*-band at ~334 nm and the *Q*-band consisting of two peaks at ~580–630 nm and at ~710 nm. The shift of the *Q*-band from ~580 nm to ~630 nm is observed in the $k(\lambda)$ spectrum of ZnPcF₄ film, which appears to be due to the effect of electron withdrawing substituents. The thickness of the ZnPc, ZnPcF₄ and mixed ZnPc/ZnPcF₄

films (Figure 4) were estimated from the ellipsometry data to be 49.2, 80.6 and 75.2 nm, respectively.

Figure 5 shows AFM images of the surface of ZnPc (a) and ZnPcF₄ (b) films as well as a film obtained by co-evaporation of ZnPc and ZnPcF₄ (1:1) (c). As can be clearly seen both ZnPc and ZnPcF₄ films exhibit a high density of azimuthally disordered roundish grains (Figure 5a), however the grain sizes of ZnPcF₄ film are noticeably smaller than those of ZnPc films (Figure 5b). The rms roughness values of ZnPc and ZnPcF₄ films were 14.2 and 6.0 nm, respectively. The film obtained by co-evaporation of ZnPc and ZnPcF₄ was smoother than the single-phase films and had the rms value 5.3 nm (Figure 5c). It is worth mentioning that the actual ratio ZnPc/ZnPcF₄ in the films

Table 1. Unit cell parameters and refinement statistics for ZnPcF₄.

Compound	ZnPcF ₄
Formula	Zn ₁ C ₃₂ N ₈ F ₄ H ₁₂
F.W.	649.87
T, K	160
System	Triclinic
Space group	<i>P</i> -1
<i>Z</i>	1
<i>a</i> , Å	3.6843(5)
<i>b</i> , Å	12.381(2)
<i>c</i> , Å	13.371(2)
α , °	88.368(5)
β , °	88.621(4)
γ , °	84.956(5)
Volume, Å ³	607.18(15)
Density (calc), g/sm ³	1.777
R ₁ (I>2 θ), %	5.19

**Figure 4.** Dispersion dependences $n(\lambda)$, $k(\lambda)$ for ZnPc (1), ZnPcF₄ (3) and mixed ZnPc/ZnPcF₄ (2) films. Thicknesses of the films (nm): 1 – 49.2, 2 – 80.6, 3 – 75.2.

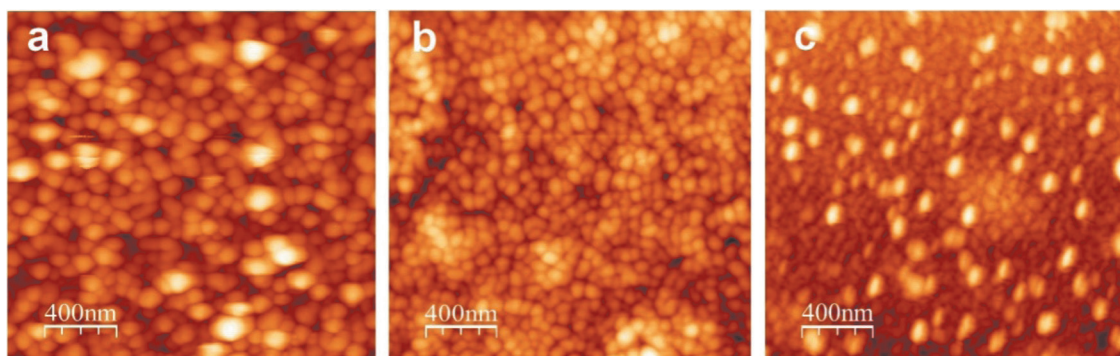
on the ITO coated glass substrate was estimated by means of XPS to be about 0.9.

X-ray diffraction patterns of thin films in the range from 5 to 30° 2 θ are shown in Figure 6. All three diffraction patterns contain a single strong diffraction peak in the 2 θ range of 6–7°, which is typical for most of M(II)Pc films^[6–7] and this usually means that the samples have a significant degree of preferred orientation relative to the substrate surface.

For ZnPc the measured interplanar distance (d) of this peak 12.69 Å noticeably differs from the position of (001) peak of β -ZnPc (d_{001} =12.54 Å).^[30] While its position does not match with the known positions of the first two diffraction peaks of α -ZnPc with d =13.0 and d =12.3 Å,^[38] some studies show that the unit cell parameters of α -ZnPc may vary significantly depending on the substrate temperature during thin film deposition process.^[39–40]

There is no information about α -ZnPc crystal structure in the literature, however the authors of works^[41–42] attribute a C2/c space group and approximate unit cell parameters a =25.9, b =3.8, c =23.9 Å and β =90.5° to α -ZnPc. Using these data, the (200) index could be assigned to the observed peak on the diffraction pattern of ZnPc thin film. The diffraction peak on the ZnPcF₄ pattern (Figure 6) is noticeably wider compared to that on the ZnPc pattern with a slight asymmetry on the right side and the maximum at 13.23 Å. Since the ZnPcF₄ powder pattern has the first two peaks with d_{001} =13.28 and d_{010} =12.36 Å relatively close to each other, it is possible to assume that ZnPcF₄ thin films consist of the same crystal phase as its polycrystalline powder, and the single observed peak is actually overlapping of the (001) and (010) peaks. The diffraction pattern of the film ZnPc/ZnPcF₄ obtained by co-evaporation of ZnPc and ZnPcF₄ powders also has a single peak, indicating that this film contains only one crystalline phase. The measured interplanar distance of this peak perfectly matches with d_{001} in the pattern of a ZnPcF₄ film (note that this value significantly differs from that for ZnPc/ZnPcF₄ thin film which was equal to 12.77 Å, as reported by Schwarze *et al.*^[23]). It is difficult to make any conclusion about the film orientation and crystal phase composition based on the position of only one diffraction peak.

In order to obtain more reliable and informative X-ray diffraction data, all three thin film samples were studied using measurements in 2D GIXD geometry. The resulting 2D diffraction patterns are shown in Figure 7. All

**Figure 5.** AFM images of the surface of ZnPc (a), ZnPcF₄ (b) and ZnPc/ZnPcF₄ (c) films.

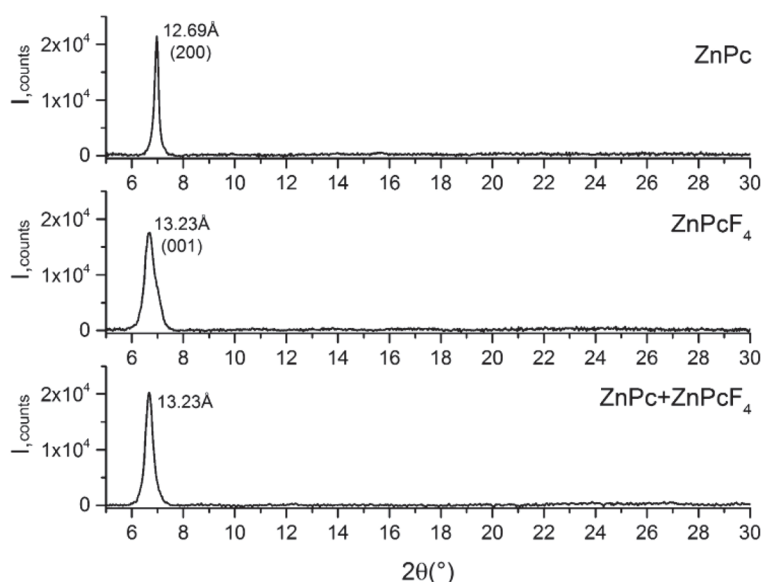


Figure 6. X-ray diffraction patterns of ZnPc, ZnPcF₄ and ZnPc/ZnPcF₄ thin films (Shimadzu XRD-7000, CuK_α-radiation, Bragg-Brentano geometry).

three samples show localized diffraction spots rather than uniform diffraction arcs, which confirms our assumption of preferential orientation of thin film samples. Each diffraction spot is characterized by 2θ position, which corresponds to a certain crystallographic plane and azimuthal angle φ (shown in Figure 7 on ZnPc diffraction pattern), which is the angle between the corresponding crystallographic plane and the substrate surface.^[28] Since the azimuthal angle φ is equal to 0° for the plane of the preferred orientation of crystallites, it means that it is parallel to the substrate surface. Therefore the measured azimuthal position of the individual diffraction spot effectively shows the angle between a corresponding crystallographic plane and a preferred orientation plane.

The white arrow on the ZnPc pattern shows a zero position for φ angle, thus the displayed φ range of each 2D GIXD pattern is $\pm 90^\circ$. The fact that each diffraction pattern has only one diffraction spot at $\varphi=0^\circ$ indicates

that all three samples have only one direction of the preferred orientation. On the diffraction pattern of ZnPc film the first diffraction ring contains two localized maximums: one in the center with $d_{200}=12.75 \text{ \AA}$ and the other at about 90° with $d_{002}=12.68 \text{ \AA}$. The presence of these two peaks proves that ZnPc film contains a crystalline phase different from β -ZnPc, since the (001) peak of β -ZnPc has only one equivalent Friedel pair ((001) and (00-1)) and thus would look like a single diffraction spot on the 2D GIXD pattern. Other diffraction arcs on the ZnPc pattern have several local maximums, however all maximums on the same ring have the same (or indistinguishably close) interplanar distances. All measured d with the assigned hkl indexes are listed in Table 2 in comparison with β -ZnPc and α -ZnPc.^[30,38]

The ZnPcF₄ pattern (Figure 7) shows more localized albeit blurry diffraction spots, meaning that ZnPcF₄ film has the preferred orientation along (001) plane and lower degree of crystallinity compared to a ZnPc film. All observed diffraction spots match with ZnPcF₄ crystal structure data. The 2D GIXD pattern of the mixed ZnPc/ZnPcF₄ film (Figure 7c) looks almost similar to that of ZnPcF₄, but with the clearer diffraction spots. 2θ and φ positions of the spots match with those of ZnPcF₄, which means that crystal structure of the mixed ZnPc/ZnPcF₄ film is very close or identical to ZnPcF₄. Therefore it is possible to assign hkl indexes to all visible diffraction spots by analogy with the ZnPcF₄ film pattern.

Figure 8 compares azimuthal profiles of diffraction spots (200) for ZnPc and (001) for ZnPcF₄ and ZnPc/ZnPcF₄ films in the φ range of -30° to 30° . Since all three films have preferred orientation along the selected plane, the azimuthal profile of the respective diffraction spot effectively shows the distribution of crystallites over the inclination angles relative to the substrate surface.

The fitting procedure of azimuthal profile using a Voigt function gives the values of FWHM 14.04, 16.02 and 12.50° for ZnPc, ZnPcF₄ and ZnPc/ZnPcF₄ films, respectively.

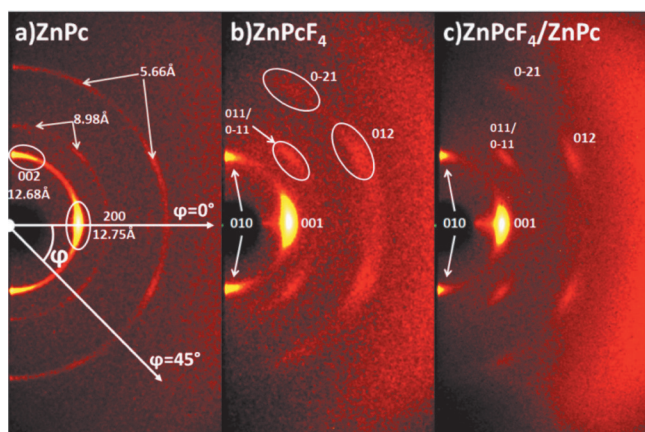
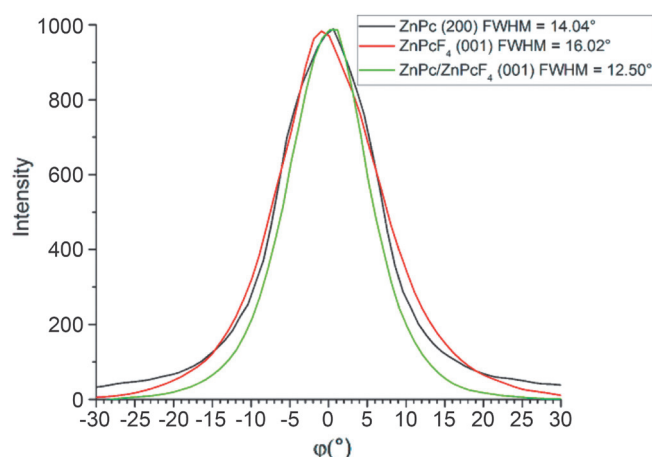


Figure 7. 2D GIXD patterns (80 mm sample-to-detector distance, CuK_α, 0.3° primary beam angle of incidence) for (a) ZnPc, (b) ZnPcF₄ and (c) ZnPc/ZnPcF₄ films.

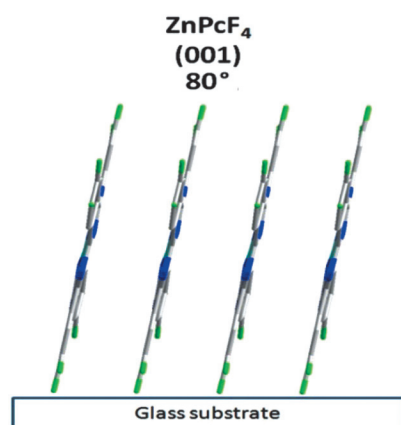
Table 2. Measured interplanar distances (d) of ZnPc thin film compared to polycrystalline sample and literature data.

ZnPc thin film, d (Å)	ZnPc powder, d (Å)	β -ZnPc, d (Å) ^[30]	α -ZnPc, d (Å) ^[38]
12.75	12.56	12.54	13.0
12.68	9.51	9.48	12.3
8.98	8.31	8.31	10.1
6.33	7.01	6.99	9.54
5.66	6.28	6.27	8.90
	5.72	5.72	5.70

**Figure 8.** Azimuthal profiles of (200) peak for ZnPc and (001) peaks for ZnPcF₄ and ZnPc/ZnPcF₄ films.

This means that the ZnPc/ZnPcF₄ film has the best ordering among these three samples. It is necessary to mention that in the case of ZnPc film the (200) peak profile does not reach zero intensity at $\pm 30^\circ \phi$ (Figure 8). This fact indicates that the ZnPc film has a significant portion of completely disordered crystallites.

Since crystal structure and preferred orientations for ZnPcF₄ are known, it is possible to calculate the angle between substrate surface and phthalocyanine macrocycles (Figure 9). The inclination angle is equal to 80° with

**Figure 9.** Orientation of ZnPcF₄ molecules relative to the substrate surface.

the deviation of $\pm 16.0^\circ$ as calculated from the azimuthal profile (Figure 8). The same inclination angle is also observed in the case of ZnPc/ZnPcF₄ film but with the less ($\pm 12.5^\circ$) deviation from the mean value. For comparison, the inclination angle of β -ZnPc film is 76.3° , as calculated from the structural data.

Conclusions

In this work, zinc phthalocyanine ZnPc, tetrafluorosubstituted zinc phthalocyanine ZnPcF₄ and mixed 1:1 ZnPc/ZnPcF₄ thin films were deposited by organic molecular beam deposition and studied to reveal the effects of F-substituents on the ZnPcF₄ films structure. The crystal structure of the ZnPcF₄ single crystal has been determined for the first time. ZnPcF₄ is shown to crystallize in the triclinic *P-1* space group, forming stacks of molecules in columnar arrangement; the unit cell parameters are $Z=1$, $a=3.6843(5)$ Å, $b=12.381(2)$ Å, $c=13.371(2)$ Å, $\alpha=88.368(5)^\circ$, $\beta=88.621(4)^\circ$, $\gamma=84.956(5)^\circ$. A combination of spectral ellipsometry, atomic force microscopy and diffraction techniques have been used to elucidate the structural features and molecular orientation of thin films. It has been shown that co-evaporation of ZnPc and ZnPcF₄ results in the formation of single-phase thin film with crystal structure identical to ZnPcF₄. Both ZnPcF₄ and ZnPc/ZnPcF₄ films have a preferred orientation along (001) plane with inclination angle of molecules relative to the substrate surface equal to 80° and the lower degree of crystallinity compared to the ZnPc film.

Acknowledgements. The authors acknowledge FASO of Russian Federation for a financial support (project 0300-2016-0007).

References

- Bouvet M., Gaudillat P., Suisse J.-M. *J. Porphyrins Phthalocyanines* **2013**, *17*, 913–919.
- van Staden J.(K.)F. *Talanta* **2015**, *14*, 75–88.
- Chen Y., Xiao Y., Su Z., Shao X., Wang S., Li X. *Mater. Lett.* **2017**, *191*, 17–21.
- Shao X., Wang S., Li X., Su Z., Chen Y., Xiao Y. *Dyes Pigments* **2016**, *132*, 378–386.
- Sun Y., Li X., Wang S., Zhang L., Ma F. *Mater. Trans.* **2017**, *58*, 103–106.
- Klyamer D.D., Sukhih A.S., Krasnov P.O., Gromilov S.A., Morozova N.B., Basova T.V. *Appl. Surf. Sci.* **2016**, *372*, 79–86.

7. Sukhikh A.S., Klyamer D.D., Parkhomenko R.G., Krasnov P.O., Gromilov S.A., Hassan A.K., Basova T.V. *Dyes Pigments* **2018**, *149*, 348–355.
8. Klyamer D.D., Sukhikh A.S., Gromilov S.A., Krasnov P.O., Basova T.V. *Sensors* **2018**, *18*, 2141.
9. Ye R., Baba M., Oishi Y., Mori K., Suzuki K. *Appl. Phys. Lett.* **2005**, *86*, 253505.
10. Ye R., Baba M., Suzuki K., Mori K. *Appl. Surf. Sci.* **2008**, *254*, 7885–7888.
11. Jiang H., Hu P., Ye J., Li Y., Li H., Zhang X., Li R., Dong H., Hu W., Kloc C. *Adv. Mater.* **2017**, *29*, 1605053.
12. Yoon S.M., Song H.J., Hwang I.-C., Kim K.S., Choi H.C. *Chem. Commun.* **2010**, *46*, 231–233.
13. Pandey P.A., Rochford L.A., Keeble D.S., Rourke J.P., Jones T.S., Beanland R., Wilson N.R. *Chem. Mater.* **2012**, *24*, 1365–1370.
14. Jiang H., Ye J., Hu P., Wei F., Du K., Wang N., Ba T., Feng S., Kloc C. *Sci. Reports* **2014**, *4*, 7573.
15. de Oteyza D.G., Barrera E., Osso J.O., Sellner S., Dosch H. *J. Am. Chem. Soc.* **2006**, *128*, 15052–15053.
16. Engel M.K. Single-Crystal Structures of Phthalocyanine Complexes and Related Macrocycles. In: *The Porphyrin Handbook* (Kadish K.M., Smith K.M., Guillard, Eds.) San Diego: Academic Press, **2003**. p. 1–242.
17. Kuzumoto Y., Matsuyama H., Kitamura M. *Jpn. J. Appl. Phys.* **2014**, *53*, 04ER16.
18. Yang J., Yim S., Jones T.S. *Sci. Reports* **2015**, *5*, 9441.
19. Hesse K., Schlettwein D. *J. Electroanal. Chem.* **1999**, *476*, 148–158.
20. Schollhorn B., Germain J.P., Pauly A., Maleysson C., Blanc J.P. *Thin Solid Films* **1998**, *326*, 245–250.
21. Ma X., Chen H., Shi M., Wu G., Wang M., Huang J. *Thin Solid Films* **2005**, *489*, 257–261.
22. Brinkmann H., Kelting C., Makarov S., Tsaryova O., Schnurpfeil G., Wöhrle D., Schlettwein D. *Phys. Status Solidi A* **2008**, *205*, 409–420.
23. Schwarze M., Tress W., Beyer B., Gao F., Scholz R., Poelking C., Ortstein K., Günther A.A., Kasemann D., Andrienko D., Leo K. *Science* **2016**, *352*, 1446–1449.
24. Peisert H., Knupfer M., Fink J. *Synth. Met.* **2003**, *137*, 869–870.
25. Peisert H., Knupfer M., Fink J. *Surf. Sci.* **2002**, *515*, 491–498.
26. Spesivtsev E.V., Rykhlytskii S.V., Shvets V.A. *Optoelectron. Instrum. Data Process.* **2011**, *47*, 419–425.
27. Tompkins H.G., Irene E.A. *Handbook of Ellipsometry*. New York: William Andrew Publishing, **2005**. 886 p.
28. Sukhikh A.S., Basova T.V., Gromilov S.A. *Acta Phys. Pol., A* **2016**, *130*, 889–891.
29. Sukhikh A.S., Basova T.V., Gromilov S.A. *J. Struct. Chem.* **2017**, *58*, 953–963.
30. Scheidt W.R., Dow W. *J. Am. Chem. Soc.* **1977**, *99*, 1101–1104.
31. *Bruker Advanced X-Ray Solutions*, Madison, Wisconsin, USA.
32. Dolomanov O.V., Bourhis L.J., Gildea R.J., Howard J.A.K., Puschmann H. *J. Appl. Cryst.* **2009**, *42*, 339–341.
33. Sheldrick G.M. *Acta Cryst. A* **2015**, *A71*, 3–8.
34. Sheldrick G.M. *Acta Cryst. C* **2015**, *C71*, 3–8.
35. Ballirano P., Caminiti R., Ercolani C., Maras A., Orru M.A. *J. Am. Chem. Soc.* **1998**, *120*, 12798–12807.
36. Novotny M., Bulir J., Bensalah-Ledoux A., Guy S., Fitl P., Vrnata M., Lancok J., Moine B. *Appl. Phys. A* **2014**, *117*, 377–381.
37. Rand B.P., Cheyng D., Vasseur K., Giebink N.C., Mothy S., Yi Y., Coropceanu V., Beljonne D., Cornil J., Bredas J.-L., Genoe J. *Adv. Funct. Mater.* **2012**, *22*(1), 1–9.
38. Kobayashi T., Uyeda N., Suito E. *J. Phys. Chem.* **1968**, *72*, 2446–2456.
39. Kment S., Kluson P., Drobek M., Kuzel R., Gregora I., Kohout M., Hubicka Z. *Thin Solid Films* **2009**, *517*, 5274–5279.
40. Senthilarasu S., Hahn Y.B., Lee S.-H. *J. Mater. Sci. – Mater. Electron.* **2008**, *19*, 482–486.
41. Zanolini A.A., Volpati D., Olivati C.A., Job A.E., Constantino C.J.L. *J. Phys. Chem. C* **2010**, *114*, 12290–12299.
42. Ashida M., Uyeda N., Suito E., Bull E. *Chem. Soc. Jpn.* **1966**, *39*, 2616–2624.

Received 16.07.2018

Accepted 10.10.2018